

Mesoporous Titanosilicate Molecular Sieves Prepared at Ambient Temperature by Electrostatic (S^+I^- , $S^+X^-I^+$) and Neutral (S^0I^0) Assembly Pathways: A Comparison of Physical Properties and Catalytic Activity for Peroxide Oxidations

Wenzhong Zhang,[†] Michael Fröba,^{‡,§} Jialiang Wang,[†] Peter T. Tanev,[†] Joe Wong,[§] and Thomas J. Pinnavaia^{*,†}

Contribution from the Department of Chemistry and Center for Fundamental Materials Research, Michigan State University, East Lansing, Michigan 48824, Institute of Inorganic and Applied Chemistry, University of Hamburg, Martin-Luther-King-Platz 6, D-20146 Hamburg, Germany, and Lawrence Livermore National Laboratory, University of California, Livermore, California 94551

Received February 23, 1996[⊗]

Abstract: Hexagonal mesoporous titanosilicates with distinguishable framework charges and textural mesoporosity, namely, Ti-MCM-41 and Ti-HMS, were prepared at ambient temperature by electrostatic and neutral assembly processes, respectively. Titanium incorporation at the 2 mol % level for both materials was accompanied by increases in lattice parameters and wall thicknesses, but the framework pore sizes remained unaffected. Cross-linking of the anionic framework of as-synthesized Ti-substituted MCM-41 prepared by electrostatic S^+I^- and $S^+X^-I^+$ assembly pathways (where S^+ is a quaternary ammonium surfactant and I^- and I^+ are ionic silicon precursors) was enhanced significantly by Ti substitution, as judged by ^{29}Si MAS NMR. The neutral framework of as-synthesized Ti-HMS formed by S^0I^0 assembly (where S^0 is a primary amine and I^0 is a neutral silicon precursor) exhibited the same high degree of cross-linking as the unsubstituted silica analog. UV–vis and XANES spectra for the calcined forms of Ti-MCM-41 and Ti-HMS indicated (i) the presence of site-isolated Ti species in the framework, (ii) predominantly tetrahedral coordination for Ti, along with some rehydrated five- and six-coordinated sites, and (iii) Ti siting that was virtually independent of the framework assembly pathway. All mesoporous molecular sieves exhibited catalytic activities superior to that of titanium silicalite for the liquid phase peroxide oxidations of methyl methacrylate, styrene, and 2, 6-di-*tert*-butylphenol. The exceptional catalytic activity in the case of Ti-HMS, especially toward larger substrates, was attributable to the small crystallite size and complementary textural mesoporosity that facilitates substrate access to framework Ti sites.

Introduction

Titanium silicalite-1 (denoted TS-1) is an effective catalyst for the liquid phase peroxide oxidations of alcohols and alkanes,¹ the epoxidation of alkenes,² and the hydroxylation of aromatics.³ The activity of TS-1 arises from the presence of accessible, site-isolated Ti centers in the silicalite framework that are capable of undergoing a facile coordination change and forming an active peroxo–titanium complex.⁴ Because of the small pore size of the inorganic framework, the substrates that can be oxidized by TS-1 are limited to species having kinetic diameters $<6 \text{ \AA}$. However, the recently reported hexagonal mesoporous silica molecular sieves prepared by electrostatic^{5,6} and neutral^{7,8} surfactant templating pathways offer promising opportunities for

the preparation of large-pore TS-1 analogs capable of transforming larger organic molecules.

MCM-41 silicas normally are prepared by one of two possible electrostatic assembly pathways. The S^+I^- pathway originally utilized by Mobil researchers⁵ involves electrostatic interactions and charge matching between positively charged assemblies of rodlike micelles of quaternary ammonium surfactants (S^+) and anionic silicate species (I^-). The second pathway, the so-called counterion-mediated $S^+X^-I^+$ pathway,⁶ makes use of the same surfactant cations under strongly acidic conditions in order to assemble positively charged silica precursors (I^+). In contrast, HMS silicas are special members of the MCM-41 class of materials prepared by a neutral S^0I^0 assembly pathway that involves hydrogen-bonding interactions between neutral S^0 primary amine surfactants and neutral I^0 inorganic precursors (e.g., tetraethyl orthosilicate).⁷ The electrostatic assembly pathways afford as-synthesized MCM-41 materials with negatively charged framework walls, whereas neutral assembly yields HMS silicas with *neutral* frameworks and walls that are

* To whom correspondence should be addressed.

[†] Michigan State University.

[‡] University of Hamburg.

[§] University of California.

[⊗] Abstract published in *Advance ACS Abstracts*, September 1, 1996.

(1) (a) Huybrechts, D. R. C.; De Bruycker, L.; Jacobs, P. A. *Nature* **1990**, *345*, 240. (b) Esposito, A.; Neri, C.; Buonomo, F. US Patent 4,480,135, 1984.

(2) Clerici, M. G.; Romano, U. US Patent 4,937,216, 1990.

(3) Taramasso, M.; Perego, G.; Notari, B. US Patent 4,410,501, 1983.

(4) (a) Notari, B. *Stud. Surf. Sci. Catal.* **1988**, *37*, 413. (b) Anpo, M.; Nakaya, H.; Kodama, S.; Kubokawa, Y. *J. Phys. Chem.* **1986**, *90*, 1633.

(5) (a) Kresge, C. T.; Leonowicz, M. E.; Roth W. J.; Vartuli, J. C.; Beck, J. S. *Nature* **1992**, *359*, 710. (b) Beck, J. S.; Vartuli, J. C.; Roth, W. J.; Leonowicz, M. E.; Kresge, C. T.; Schmitt, K. D.; Chu, C. T.-W.; Olson, D. H.; Sheppard, E. W.; McCullen, E. B.; Higgins, J. B.; Schlenker, J. L. J. *Am. Chem. Soc.* **1992**, *114*, 10834.

(6) (a) Huo, Q.; Margolese, D. I.; Ciesla, U.; Feng, P.; Gier, T. E.; Sieger, P.; Leon, R.; Petroff, P. M.; Schüth, F.; Stucky, G. D. *Nature* **1994**, *368*, 317. (b) Huo, Q.; Margolese, D. I.; Ciesla, U.; Demuth, D. G.; Feng, P.; Gier, T. E.; Sieger, P.; Firouzi, A.; Chmelka, B. F.; Schüth, F.; Stucky, G. D. *Chem. Mater.* **1994**, *6*, 1176.

(7) Tanev, P. T.; Pinnavaia, T. J. *Science* **1995**, *267*, 865.

(8) (a) Bagshaw, S. A.; Prouzet, E.; Pinnavaia, T. J. *Science* **1995**, *269*, 1242. (b) Attard, G. S.; Glyde, J. C.; Göltner, C. G. *Nature* **1995**, *378*, 366.

characteristically thicker than those formed by electrostatic assembly. These fundamental differences give rise to distinguishable physical and chemical properties for MCM-41 and HMS materials.

Corma *et al.* have reported the preparation and catalytic activity of Ti-MCM-41.⁹ The catalyst was obtained by electrostatic S⁺I⁻ assembly under hydrothermal conditions at 408 K. We reported the *ambient temperature* preparation of S⁺X⁻I⁺-assembled Ti-MCM-41 and S^oI^o-assembled Ti-HMS catalysts¹⁰ and found preliminary evidence for greater reactivity for the Ti-HMS derivative. More recently, several other groups have reported the preparation and catalytic properties of Ti-MCM-41.^{11–15} In all instances the syntheses were accomplished using exclusively the S⁺I⁻ assembly pathway⁵ under hydrothermal conditions at temperatures above 373 K. Thus, relatively little is known concerning the catalytic activities of titanium-substituted mesoporous molecular sieves assembled at ambient temperature by electrostatic assembly pathways.

In the present work we investigate the synthesis of mesoporous Ti-MCM-41 and Ti-HMS catalysts *via* electrostatic and neutral assembly processes at *ambient temperature*, compare the physical properties of these products, and elucidate the differences in their catalytic activities for the peroxide oxidations of large organic molecules.

Experimental Section

Materials. TS-1 with an analytically determined titanium loading of 2 mol % was synthesized by the method of Taramasso *et al.*³ Tetraethyl orthosilicate (TEOS), tetraisopropyl orthotitanate (TIPOT), and tetrapropylammonium hydroxide (TPAOH) were used as a source of silica, titanium, and template, respectively. The molar composition of the reaction mixture was 0.022 Ti:1.0 Si:0.35 TPAOH:35 H₂O. The synthesis was accomplished by placing the reaction mixture in a autoclave and heating at 443 K for 48 h under static conditions.

Ti-MCM-41 and Ti-HMS derivatives with equivalent titanium loadings (i.e., ~2 mol %) were prepared using deionized colloidal silica or TEOS as the source of silica, TIPOT as a titanium precursor, and long-chain alkylammonium or alkylamine surfactants, respectively, as templates. In contrast to the hydrothermal reaction conditions normally used to prepare Ti-MCM-41 (i.e., autoclaving above 373 K), our Ti-MCM-41 catalysts were prepared by *ambient temperature synthesis* via electrostatic S⁺I⁻ and S⁺X⁻I⁺ assembly. In both of these electrostatic pathways cetyltrimethylammonium cations (CTMA⁺) served as the template. For S⁺I⁻ assembly, a deionized 34 wt % colloidal silica solution (Aldrich) and TIPOT were added to a solution of template under vigorous stirring and the pH of the reaction mixture was adjusted to 12 with tetramethylammonium hydroxide (TMAOH). The molar composition of the reaction mixture was 0.020 Ti:1.0 Si:0.50 CTMA⁺:1.0 TMAOH:160 H₂O. The preparation of Ti-MCM-41 by the counterion-mediated pathway (S⁺X⁻I⁺) utilized strongly acidic

conditions (pH 1.5) in order to generate and assemble positively charged silicon species from TEOS. In a typical preparation the template was dissolved in acidic aqueous solution followed by the addition of a TEOS/TIPOT solution. A higher Ti:Si gel ratio of 1:10 was used for this pathway in order to prepare a product with the desired Ti:Si ratio of 2:98. The use of excess Ti for this preparation was necessitated by the high solubility of Ti under strongly acidic conditions. The composition of the reaction mixture was 0.10 Ti:1.0 Si:0.20 CTMA⁺:1.0 HCl:160 H₂O. For both electrostatic pathways, the reaction mixture was aged under vigorous stirring for 24 h in order to obtain the crystalline Ti-MCM-41 product.

Ti-HMS was synthesized via a neutral S^oI^o templating pathway using dodecylamine (DDA) as the surfactant and ethanol (EtOH) as a cosolvent. In a typical preparation the TEOS/TIPOT solution was added to the solution of DDA in water and ethanol under vigorous stirring. The molar composition of the reaction mixture was 0.022 Ti:1.0 Si:0.20 DDA:9.0 EtOH:160 H₂O. The reaction mixture was aged at ambient temperature under vigorous stirring for 24 h in order to obtain the crystalline product. For comparative purposes we have also prepared pure silica MCM-41 and HMS samples by omitting the Ti source in the above preparations. All samples were filtered, washed thoroughly with water, dried at ambient temperature, and calcined at 923 K for 4 h.

Commercially available samples of MgTiO₃, anatase, rutile, and neptunite and a sample of hexadecaphenyl octasiloxyspiro(9,9)titanate (denoted spiro titanate¹⁶) were used as reference materials for XANES analysis. Spirotitanate contains Ti atoms tetrahedrally coordinated to four siloxy oxygens.¹⁷

Characterization. The powder X-ray diffraction (XRD) patterns of all samples were measured on a Rigaku Rotaflex diffractometer equipped with a rotating anode and CuK α radiation ($\lambda = 1.542 \text{ \AA}$). In general, the diffraction data were collected by using a continuous scan mode with a scan speed of 2 deg (2 Θ)/min.

²⁹Si MAS NMR spectra were measured at 79.5 MHz on a Varian VXR-400S solid state NMR spectrometer equipped with a magic angle spin probe. For each measurement the samples were placed in zirconia rotors and spun at 4.2 kHz. The quantitative determination of Q², Q³, and Q⁴ sites was accomplished by deconvolution of the spectra.

UV-vis spectroscopic measurements were carried out on a Shimadzu UV-3101PC UV-vis-near-IR scanning spectrophotometer equipped with an integrating sphere. A reflection mode with a resolution of 10 \AA and BaSO₄ reference were used for the measurements. The collected relative reflection intensity ($R_{\infty} = R_{\text{sample}}/R_{\text{reference}}$) was transformed into $F(R_{\infty})$ by using the Kubelka-Munk function $F(R_{\infty}) = (1 - R_{\infty})^2/(2R_{\infty})$.¹⁸ All spectra were plotted in terms of $F(R_{\infty})$ versus wavelengths.

The X-ray absorption spectra were recorded at the Stanford Synchrotron Radiation Laboratory with a SPEAR storage ring operating at 3 GeV and 50–100 mA. Wiggler beam line 10-2 was used with a Si(220) double-crystal monochromator. In order to reduce contributions from higher harmonics, the second monochromator crystal was detuned to 50% of the maximum intensity. The slit before the monochromator as well as that in front of the first ion chamber was set to 1 mm height. The energy calibration of the monochromator was checked between every two spectra by measuring the Ti K-edge (4966 eV) of a Ti metal foil reference. All spectra were recorded at room temperature using a continuous scan technique (QEXAFS).¹⁹ The counting time per data point was 0.5 s, and the distance between data points was 0.2 eV.²⁰ The pre-edges were normalized for absorbance by fitting the spectral region from 4900 to 4950 eV with a Victoreen function and subtracting this as background absorption. In addition, all spectra were normalized for atomic absorption by using the average absorption coefficient of the region from 5050 to 5150 eV. The normalizations were performed in order to compare the pre-edge peak intensities, energy positions, and peak widths. The normalized Ti K-edge XANES spectra were fitted in the energy range of 4960–4980 eV using a series of symmetric profile functions. Lorentzian and Gaussian functions were used for

(9) Corma, A.; Navarro, M. T.; Perez-Pariente, T. *J. Chem. Soc., Chem. Commun.* **1994**, 147.

(10) (a) Tanev, P. T.; Chibwe, M.; Pinnavaia, T. J. *Nature* **1994**, 368, 321. (b) Pinnavaia, T. J.; Tanev, P. T.; Wang, J.; Zhang, W. In *Advances in Porous Materials*; Komarneni, Sh., Beck, J. S., Smith, D. M., Eds.; MRS Symposium Proceedings Series; MRS: Pittsburgh, 1995; Vol. 371, p 53.

(11) Franke, O.; Rathousky, J.; Schulz-Ekloff, G.; Starek, J.; Zukal, A. *Zeolite and Related Microporous Materials: State of the Art 1994*. In *Studies in Surface Science and Catalysis*; Weitkamp, J., Karge, H. G., Pfeifer, H., Holderich, W., Eds.; Elsevier Science BV: Amsterdam, 1994; vol. 84, p 77.

(12) (a) Sankar, G.; Rey, F.; Thomas, J. M.; Greaves, G. N.; Corma, A.; Dobson, B. R.; Dent, A. J. *J. Chem. Soc., Chem. Commun.* **1994**, 2279. (b) Maschmeyer, T.; Rey, F.; Sankar, G.; Thomas, J. M. *Nature* **1995**, 378, 159.

(13) Blasco, T.; Corma, A.; Navarro, M. T.; Pariente, J. P. *J. Catal.* **1995**, 156, 65.

(14) Reddy, J. S.; Dicko, A.; Sayari, A. *Third International Symposium on Synthesis of Zeolites and Expanded Layered Compounds*, Anaheim, CA, 1995; in press.

(15) Gontier, S.; Tuel, A. *J. Catal.* **1995**, 157, 124.

(16) Zeidler, V. A.; Brown, C. A. *J. Am. Chem. Soc.* **1957**, 79, 4618.

(17) Hursthouse, M. B.; Hossain, M. A. *Polyhedron* **1984**, 3, 95.

(18) Kortum, G. *Reflectance Spectroscopy*; Springer-Verlag: New York, 1969.

(19) Frahm, R. *Nucl. Instrum. Methods Phys. Res.* **1988**, A270, 578.

(20) Frahm, R.; Wong, J. *J. Appl. Phys.* **1993**, 32, 188.

Table 1. Properties of Ti-Substituted Mesoporous Silicas Prepared by Ambient Temperature Synthesis Using Different Templating Pathways

parameter ^a	MCM-41 (S ⁺ I ⁻)	MCM-41 (S ⁺ X ⁻ I ⁺)	HMS (S ⁰ I ⁰)
surfactant	C ₁₆ H ₃₃ N(CH ₃) ₃ ⁺	C ₁₆ H ₃₃ N(CH ₃) ₃ ⁺	C ₁₂ H ₂₅ NH ₂
Ti:Si ratio (mol)			
initial gel	2.0:98	10:90	2.2:97.8
calcined product	2.2:97.8	2.5:97.5	2.4:97.6
<i>d</i> ₁₀₀ (Å)	38.1 (36.0)	36.5 (33.0)	40.2 (36.0)
unit cell (Å)	44.0 (41.5)	42.5 (38.1)	46.4 (41.5)
Δ (Å)	4.1 (8.5)	5.6 (9.6)	0 (3.0)
H–K pore size (Å)	29 (28)	27 (26)	27 (26)
FWT (Å)	15 (12)	15 (12)	19 (15)
S _{BET} (m ² /g)	859 (923)	1354 (1345)	1075 (1108)
V _{total} (cm ³ /g)	0.70 (0.72)	0.92 (0.95)	1.40 (1.42)
V _{fr} (cm ³ /g)	0.68 (0.70)	0.90 (0.92)	0.68 (0.70)
V _{tx} (cm ³ /g)	0.02 (0.02)	0.02 (0.03)	0.72 (0.72)
V _{tx} /V _{fr}	0.03 (0.03)	0.02 (0.03)	1.06 (1.03)

^a The unit cell parameter is $2d_{100}/\sqrt{3}$, and Δ is the unit cell contraction upon calcination. FWT is the framework wall thickness obtained by subtracting the Horvath–Kawazoe (H–K) pore size from the unit cell parameter. The total liquid pore volume, V_{total}, was estimated at a relative pressure of 0.95 assuming full surface saturation. The volume of framework-confined mesopores, V_{fr}, was determined from the upper inflection point of the corresponding adsorption step. The volume of textural mesopores, V_{tx}, was obtained from the equation $V_{tx} = V_{total} - V_{fr}$. The data in parentheses are for the pure silica analogs.

fitting the pre-edge and the ascending absorption edge features, respectively. The XANES data of the micro- and mesoporous titanosilicates were collected in the fluorescence-yield mode, using a Stern–Heald type detector filled with Ar gas,²¹ whereas all reference compounds were measured in a transmission mode using two ion chambers. The first chamber was filled with a mixture of He and N₂ (ratio 2:1) and the second only with N₂.

Nitrogen adsorption-desorption measurements were carried out at 77 K on a Coulter Omnisorp 360CX Sorptometer using a continuous flow measurement mode. Prior to the measurements, samples were outgassed at 423 K and 10⁻⁶ Torr for 12 h. The pore size distributions were calculated by the method of Horvath–Kawazoe.²²

Catalytic Experiments. The catalytic performance of all samples was tested for the liquid phase peroxide oxidation of (i) methyl methacrylate (MMA) to methyl pyruvate, (ii) styrene to benzaldehyde, and (iii) 2,6-di-*tert*-butylphenol (2,6-DTBP) to quinones. All reactions were performed under vigorous stirring in a three-neck glass flask equipped with a condenser and thermometer. The oxidation of MMA and styrene was carried out using 10 mmol of substrate, 30 mg of catalyst, and 10 mL of acetonitrile as a solvent. The amount of 30 wt % H₂O₂, reaction temperature, and reaction time were as follows: (i) 40 mmol of H₂O₂, 321 K, and 6 h, respectively, for MMA oxidation and (ii) 20 mmol of H₂O₂, 321 K, and 3 h, respectively, for styrene oxidation. For 2,6-DTBP oxidation, however, 10 mmol of substrate, 100 mg of catalyst, 10 mL of acetone as a solvent, and 30 mmol of 30 wt % H₂O₂ were used, and the reaction was carried out at 335 K for 2 h. The products were analyzed by means of a GC equipped with a SPB-20 capillary column and a FID. The reaction products were confirmed by GC–MS analysis. The internal standard method was used for quantitative analysis of the products. The conversion of substrate and selectivities to the products were calculated through carbon balance.

Results and Discussion

Synthesis. A major objective of this study was to elucidate the structure–reactivity relationships for mesoporous MCM-41 and HMS titanosilicates prepared at ambient temperature by electrostatic and neutral surfactant templating pathways, respectively. In order to minimize the number of compositional and structural variables for these two classes of materials and to focus on potential differences in local Ti siting by XANES spectroscopy, the *ambient temperature* synthesis was performed in such a way that the Ti loading for the two classes of materials was ~2 mol % and the framework-confined mesopore size was

27–29 Å. Cetyltrimethylammonium cations were used as the templating surfactant for both S⁺I⁻ and S⁺X⁻I⁺ electrostatic preparations.

The *ambient temperature* synthesis of Ti-HMS materials by the neutral S⁰I⁰ approach generally affords materials with larger framework-confined pores than the corresponding S⁺I⁻ or S⁺X⁻I⁺ pathways with surfactants of the same alkyl chain lengths. Thus, in order to prepare Ti-HMS with an average pore size of 27 Å, we selected a primary amine template with a shorter alkyl chain, namely, dodecylamine. In all cases, template removal was accomplished by calcination in air at 923 K for 4 h.

Characterization. (a) XRD. Table 1 summarizes the properties of the Ti-MCM-41 and Ti-HMS catalysts prepared by different templating pathways. Included in the table for comparison are the structural parameters for the pristine silicates (the values in parentheses). It should be noted that both S⁺I⁻ and S⁰I⁰ pathways, allow for the essentially complete incorporation of the Ti in the product at the 2 mol % level, whereas the S⁺X⁻I⁺ pathway required a 4-fold excess of Ti in the reaction mixture in order to achieve a similar Ti loading (2.5 mol %). In addition, the yields of crystalline product (based on Si) for the S⁺I⁻ and S⁰I⁰ pathways were more than 85%, whereas that for the S⁺X⁻I⁺ pathway was only about 50%.

All reaction products exhibit similar *d*₁₀₀, unit cell parameters, and H–K pore sizes, but Ti-MCM-41 and Ti-HMS catalysts differ dramatically by their lattice contraction parameters (cf. Table 1). The significant lattice contraction exhibited by Ti-MCM-41 samples prepared by the electrostatic S⁺I⁻ and S⁺X⁻I⁺ pathways is not surprising and could be attributed to the cross-linking of the significant amount of non-fully-condensed framework silanol groups upon calcination (see below). In contrast Ti-HMS prepared by neutral templating does not exhibit lattice contraction due to its more fully cross-linked framework. We have previously noted^{7,23} that the neutral S⁰I⁰ pathway affords mesoporous materials with more fully cross-linked and thicker framework walls than the electrostatic templating pathways. We have attributed this phenomenon to the absence of surfactant–silica oligomer charge matching and silica–silica oligomer charge repulsive interactions in forming the framework walls. As shown by the data in Table 1 the framework wall thickness of all materials increases upon Ti incorporation into the framework. The changes in unit cell size and framework wall thickness (cf. Table 1) strongly suggest Ti

(21) Lytle, F. W.; Greigor, R. B.; Sandstrom, D. R.; Marques, D. R.; Wong, J.; Spiro, C. L.; Huffman, G. P.; Huggins, F. E. *Nucl. Instrum. Methods* **1984**, 226, 542.

(22) Horvath, G.; Kawazoe, K. *J. J. Chem. Eng. Jpn.* **1983**, 16, 470.

(23) Tanev, P. T.; Pinnavaia, T. J. *Chem. Mater.* **1996**, 8, 2068.

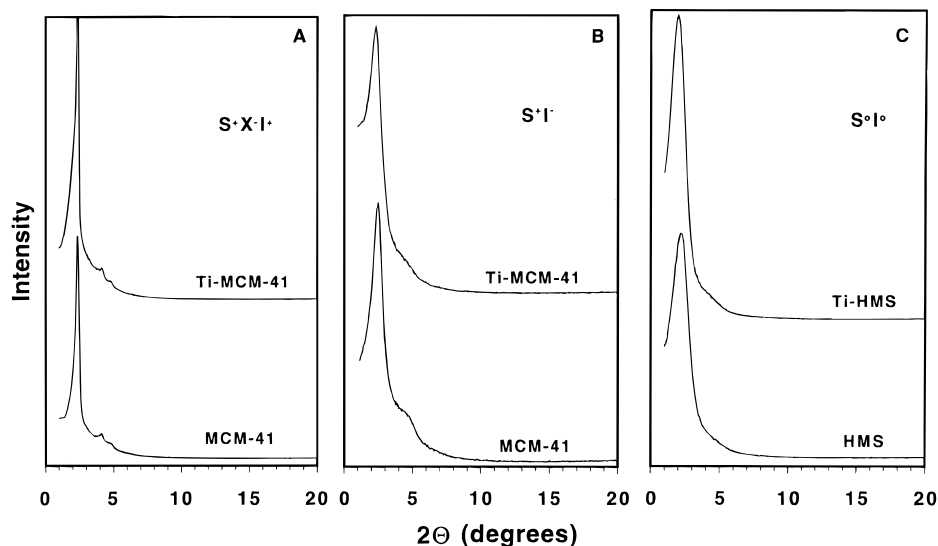


Figure 1. Powder XRD patterns for calcined pure and Ti-substituted (2 mol %) silica molecular sieves prepared at ambient temperature: (A) MCM-41 and Ti-MCM-41 prepared by $S^+X^-I^+$ assembly, (B) MCM-41 and Ti-MCM-41 prepared by S^+I^- assembly, and (C) HMS and Ti-HMS prepared by $S^\circ I^\circ$ assembly.

incorporation in the walls of the mesoporous silicate framework. An increase in the unit cell size parameter has been also noted²⁴ to occur upon Ti incorporation into ZSM-5 frameworks.

It is noteworthy that the specific surface areas are very similar for the pure and Ti-substituted derivatives. On the basis of comparisons of the full N_2 adsorption–desorption isotherms (not shown), the most significant difference between the Ti-substituted products prepared by neutral and electrostatic templating pathways is in the substantially larger textural mesoporosity exhibited by the $S^\circ I^\circ$ assembled Ti-HMS derivative (compare V_{ix} and $V_{\text{ix}}/V_{\text{fr}}$ ratios in Table 1). Ti-HMS exhibits a ratio of $V_{\text{ix}}/V_{\text{fr}}$ mesoporosity of 1.06 whereas Ti-MCM-41 samples exhibit negligible small ratios in the range of 0.02–0.03. The enhanced interparticle mesoporosity of Ti-HMS, which is a consequence of the smaller particle size afforded by neutral surfactant templating, will be shown later to play an important role in liquid phase catalytic oxidation reactions of large organic molecules.

Figure 1 illustrates the XRD patterns of the calcined Ti-MCM-41 and Ti-HMS materials together with those for the corresponding pure silica analogs. All materials exhibit well-defined 100 reflections in their XRD patterns. Hexagonal mesostructures with greater long-range order were obtained at ambient temperature conditions by the $S^+X^-I^+$ pathway (Figure 1A). This is evidenced by the presence of additional relatively narrow 110 and 200 diffraction lines in the XRD patterns of pure and Ti-substituted MCM-41 samples. The diffraction patterns of the calcined Ti-MCM-41 and pure silica analog prepared by S^+I^- pathway (Figure 1B) are very similar to those of HMS and Ti-HMS (Figure 1C). These patterns generally exhibit 100 reflections accompanied by broader, unresolved higher order reflections. These results are not surprising in view of the ambient temperature conditions used for the synthesis and the lack of NaOH in our S^+I^- reaction mixtures. We observed a similar lack of long-range order for a series of pure silica MCM-41 materials prepared at ambient temperature by the S^+I^- assembly pathway with surfactants of different alkyl chain lengths.²³ The lack of long-range order exhibited by the HMS and Ti-HMS samples was attributed to the weak H-bonding forces that govern the neutral $S^\circ I^\circ$ assembly process and to the corresponding small scattering domain sizes.⁷

(b) ^{29}Si MAS NMR. Figure 2 shows the ^{29}Si MAS NMR spectra for *as-synthesized* samples of pure and Ti-substituted mesoporous molecular sieves prepared by ambient temperature S^+I^- , $S^+X^-I^+$ and $S^\circ I^\circ$ assembly. In general, three bands centered at chemical shifts of -92 , -100 , and -110 ppm were observed for the MCM-41 derivatives. These bands can be attributed to $\text{Si}(\text{OSi})_x(\text{OH})_{4-x}$ framework units where $x = 2$ (Q^2), $x = 3$ (Q^3), and $x = 4$ (Q^4), respectively. It is noteworthy that all *as-synthesized* electrostatically-templated pure and Ti-substituted MCM-41 samples exhibit a higher fraction of incompletely cross-linked Q^2 and Q^3 framework units than the $S^\circ I^\circ$ HMS samples (see Figure 2). In addition, the *as-synthesized* pure and Ti-substituted HMS samples exhibit a much higher average ratio of $Q^4/(Q^3 + Q^2)$ units (~ 2.8) than the *as-synthesized* pure and Ti-substituted MCM-41 samples prepared by electrostatic templating (~ 1.0). This implies that neutral templating allows for the preparation of mesoporous molecular sieves with more completely cross-linked frameworks. A noteworthy trend is observed by comparing the spectra of pure and Ti-substituted MCM-41 samples prepared by both electrostatic templating pathways. Significantly, Ti incorporation leads to a dramatic increase of the cross-linking of the MCM-41 framework. This is evidenced by the increase in the fraction of Q^4 sites at the expense of both Q^2 and Q^3 framework sites. In the case of HMS, the increase of the fraction of Q^4 sites upon Ti incorporation is not as significant due to the much greater degree of cross-linking exhibited by the pure silica framework.

An additional consequence of Ti framework incorporation is the broadening of the corresponding Q^2 , Q^3 , and Q^4 peaks in the ^{29}Si MAS NMR spectra. This broadening could be attributed to the effect of the Ti sites on the chemical environment of the adjacent Si atoms.

(c) UV–Vis Diffuse Reflectance Spectroscopy. The incorporation of titanium into MCM-41 and HMS frameworks was further verified by UV–vis diffuse reflectance spectroscopy. The corresponding spectra of the Ti-substituted samples are shown in Figure 3, along with those for TS-1, HMS, and anatase. The spectrum for TS-1 shows an absorption band at 210 nm, whereas bulk titania (anatase) shows a band at 325 nm. The band at 210 nm was attributed to ligand-to-metal charge transfer associated with isolated Ti(IV) framework sites in tetrahedral coordination.²⁵ The broad absorption band centered at 325 nm

(24) van Koningsveld, H.; Jansen, J. C.; van Bekkum, H. *Zeolite* **1990**, *10*, 235.

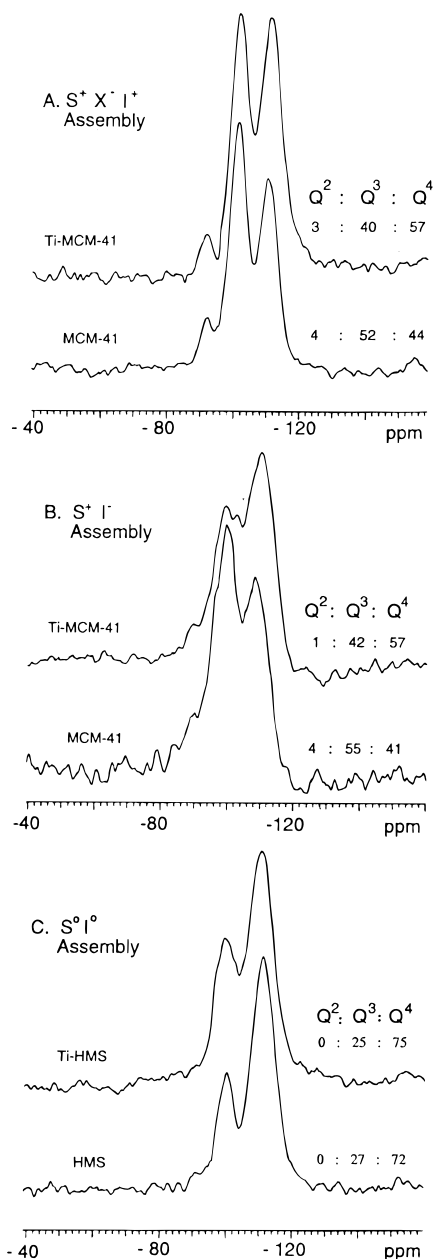


Figure 2. ^{29}Si MAS NMR spectra of as-synthesized pure and Ti-substituted (2 mol %) silica molecular sieves prepared at ambient temperature: (A) MCM-41 and Ti-MCM-41 prepared by $\text{S}^+\text{X}^-\text{I}^+$ assembly, (B) MCM-41 and Ti-MCM-41 prepared by S^+I^- assembly, and (C) HMS and Ti-HMS prepared by S^0I^0 assembly.

is typical for ligand-to-metal charge transfer occurring in bulk titania. The spectra for the mesoporous Ti-MCM-41 and Ti-HMS derivatives lack the 325 nm band characteristic for segregated titania. This suggests that most of the Ti atoms in our Ti-MCM-41 and Ti-HMS samples occupy site-isolated positions in the silica framework.

The spectra for Ti-MCM-41 and Ti-HMS are clearly different from the spectrum of the microporous TS-1. This is manifested by the much broader character of the absorption bands centered at 220 and 260–270 nm. The possibility of some Ti–O–Ti clustering in the framework cannot be unequivocally precluded as amorphous $\text{TiO}_2/\text{SiO}_2$ gels with various Ti content exhibit absorption bands in the intermediate range of 250–330 nm.⁴ However, the 220 nm band clearly signifies that much of the

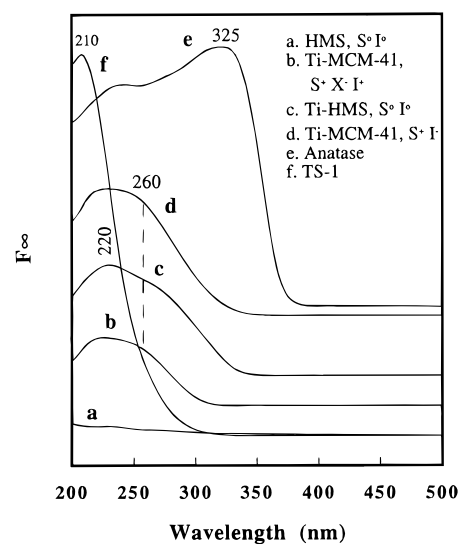


Figure 3. UV-vis spectra of calcined Ti-containing materials.

Ti is in site-isolated form. The slight shift and the increase in the width of the 220 nm band may be indicative of a Ti in a distorted tetrahedral environment or of the presence of Ti species in an octahedral coordination sphere.^{13,14} However, since there is very little shifting of the band toward lower wavelengths upon thermal dehydration, we favor a distorted tetrahedral environment for most of the Ti sites in Ti-MCM-41 and Ti-HMS. The XANES data provided below verify this assignment. We believe that this distorted environment is a direct consequence of the amorphous character of the pore walls (i.e., a wide range of Ti–O–Si bond angles).

According to several literature studies,²⁷ the absorption shoulder at 260–270 nm can be attributed to the presence of site-isolated Ti atoms in penta- or octahedral coordination. Similar UV-vis behavior, indicative of a high fraction of higher coordinated Ti sites, also has been reported to occur upon hydration of TS-1.²⁷ The presence of a significant fraction of Ti sites with coordination numbers higher than four in Ti-MCM-41 and Ti-HMS may be associated with the less crystallographic order in the pore walls, the much higher accessible surface area, and the larger mesopores. These factors most likely are responsible for the observed enhanced hydration of Ti sites in MCM-41 and HMS relative to silicalite-1.

It is important to note that the UV-vis spectra of the electrostatically templated Ti-MCM-41 and Ti-HMS prepared by neutral templating are very similar and practically indistinguishable. This implies that the effect of the templating method on the Ti siting in Ti-MCM-41 and Ti-HMS samples prepared under ambient temperature conditions is negligible. Therefore, any differences in the catalytic behavior of these materials may not be attributed to intrinsic differences in Ti siting.

(d) X-ray Absorption. In order to better elucidate the nature of the Ti sites in mesoporous Ti-MCM-41 and Ti-HMS samples, we have performed Ti K-edge XANES measurements. For comparison purposes we have also obtained Ti K-edge XANES spectra of reference compounds such as octahedrally coordinated anatase, rutile, MgTiO_3 , distorted octahedrally coordinated neptunite, tetrahedrally coordinated spiro titanate, and TS-1. Figure 4 shows the Ti K-edge XANES spectra of the reference compounds. All reference compounds with nearly octahedral Ti site symmetry exhibit multiple, low-intensity pre-edge peaks

(25) Boccuti, M. R.; Rao, K. M.; Zecchina, A.; Leofanti, G.; Petrini, G. *Stud. Surf. Sci. Catal.* **1989**, *48*, 133.

(26) Gontier, S.; Tuel, A. *Zeolites* **1995**, *15*, 601.

(27) (a) Geobaldo, C. F.; Bordiga, S.; Zecchina, A.; Giamello, E. *Catal. Lett.* **1992**, *16*, 109. (b) Bonneviot, L.; Trong On, D.; Lopez, A. *J. Chem. Soc., Chem. Commun.* **1993**, 685. (c) Trong On, D.; Denis, I.; Lortie, C.; Cartier, C.; Bonneviot, L. *Stud. Surf. Sci. Catal.* **1994**, *83*, 101.

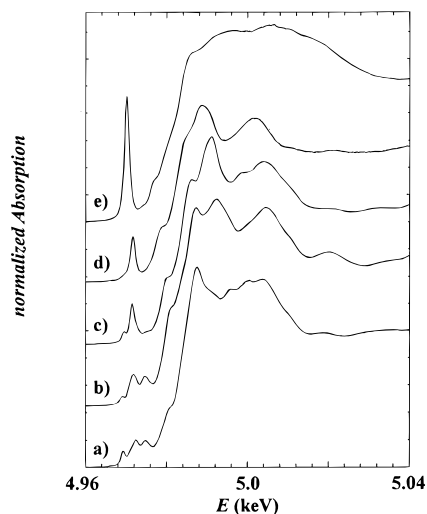


Figure 4. Normalized Ti K-edge XANES spectra of reference compounds containing Ti in tetrahedral and octahedral oxygen environments: (a) anatase, (b) rutile, (c) MgTiO₃, (d) neptunite, and (e) spirotitanate.

Table 2. Ti K-edge XANES Results for Ti-Containing Materials^a

sample	position (eV)	normalized height	FWHM ^b (eV)
spirotitanate	4969.9	0.95	0.87
rutile	4971.5	0.20	1.5
anatase	4971.7	0.15	1.7
MgTiO ₃	4971.1	0.27	0.8 ^b
neptunite	4971.2	0.33	1.2
TS-1 (2% Ti)	4970.0	0.52	1.0
Ti-MCM-41 (S ⁺ I ⁻ , 2% Ti)	4970.2	0.30	1.3
Ti-MCM-41 (S ⁺ X ⁻ I ⁺ , 2.5% Ti)	4970.3	0.31	1.3
Ti-HMS (S ⁺ I ^o , 2.4% Ti)	4970.3	0.31	1.3

^a The Ti K-edge XANES parameters were obtained by fitting the central pre-edge peak to a Lorentzian function. ^b The full width at half-maximum, FWHM, is for the central pre-edge peak.

in the region from 4960 to 4980 eV (cf. spectra a and b). Distortion of the octahedral geometry (inversion symmetry) leads to an increase in intensity of the central peak, as shown for MgTiO₃ and neptunite²⁸ (spectra c and d). In contrast, the spirotitanate with nearly regular tetrahedral geometry exhibits a single, very-high-intensity pre-edge peak (spectrum e). These results (see Figure 4 and Table 2) are in good agreement with previous studies.^{29–32} We may conclude, therefore, that tetrahedral Ti sites give a single, high-intensity pre-edge peak, whereas Ti sites in regular octahedral symmetry afford multiple, low-intensity pre-edge peaks. Although tetrahedral and highly distorted octahedral Ti sites exhibit similar single pre-edge peaks, the two environments clearly are distinguishable by means of peak intensity and position.

The Ti K-edge XANES spectra of the mesoporous Ti-MCM-41 and Ti-HMS samples prepared by electrostatic and neutral templating methods, respectively, are shown in Figure 5. Included for comparison is the spectrum for microporous TS-1. The following features are evident: (i) the spectra for all samples are very similar and contain a sharp pre-edge peak, (ii) the energy position of the pre-edge peak for Ti-substituted MCM-41 and HMS is similar to that for TS-1 and spirotitanate,

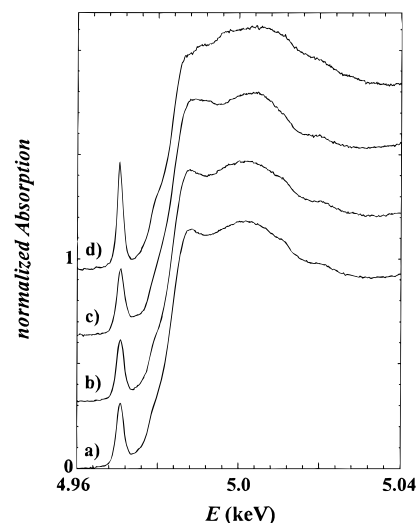


Figure 5. Normalized Ti K-edge XANES spectra of calcined (a) Ti-HMS prepared by S⁺I^o assembly, (b) Ti-MCM-41 prepared by S⁺X⁻I⁺ assembly, (c) Ti-MCM-41 prepared by S⁺I⁻ assembly, and (d) TS-1.

but different from that of the reference materials containing octahedral Ti (see Table 2), (iii) the two Ti-MCM-41 samples and Ti-HMS exhibit weaker pre-edge peaks that are slightly shifted toward higher energies and wider FWHM than those of TS-1 and spirotitanate, suggesting in addition to tetrahedral Ti the probable presence of some Ti higher coordination sites (see below), and (iv) most significantly, the spectral parameters for calcined Ti-substituted MCM-41 and HMS molecular sieves prepared via different assembly pathways at ambient temperature are very similar and practically indistinguishable. These observations are also supported by our UV-vis results and show that the Ti siting in mesoporous MCM-41 and HMS materials is independent of the templating pathway.

Extending somewhat further our interpretation of the XANES data, we note that Farges *et al.* performed ab initio multiple-scattering calculations of the Ti K-edge XANES spectra for mixtures of reference compounds containing Ti atoms with various coordination.³³ For instance, they calculated that the normalized height of the central pre-edge peak varies from 0.6 to 1.0 for 4-fold Ti, from 0.4 to 0.7 for 5-fold Ti, and from 0.05 to 0.27 for 6-fold Ti containing compounds. Besides the differences in intensity, the 4- and 6-fold Ti containing compounds were found to differ by energy position of the pre-edge peak. The energy position of the pre-edge peak for 6-fold Ti containing compounds was found to be shifted an average of 1.5 eV toward higher energies.³³ Thus, structures containing mixtures of 4-fold Ti with 5-fold or 6-fold coordinated Ti sites should exhibit pre-edge peaks with lower intensity that are slightly shifted toward higher energies. Therefore, the coordination state of Ti-sites in our Ti-MCM-41 and Ti-HMS materials may well be a mixture of 4-, 5-, and 6-fold coordinations, with tetrahedral coordination being in the majority. The higher coordination Ti sites are most likely generated through hydration of the tetrahedrally coordinated sites.

Catalytic Results. Corma *et al.* have demonstrated⁹ that Ti-MCM-41 catalyzes the epoxidation of rather small organic molecules such as hex-1-ene and norbornene. We have reported that Ti-MCM-41 and Ti-HMS are very effective oxidation catalysts for bulky aromatic molecules that can not be converted over TS-1, such as 2,6-DTBP.¹⁰ More recently, several groups have elaborated on the preparation, characterization and catalytic activity of Ti-MCM-41^{11–15} and Ti-HMS.^{15,34} All of the Ti-

(28) Cannillo, E.; Mazzi, F.; Rossi, G. *Acta Crystallogr.* **1966**, *21*, 200.

(29) Waychunas, G. A. *Am. Mineral.* **1987**, *72*, 89.

(30) Behrens, P.; Felsche, J.; Vetter, S.; Schulz-Ekloff, G.; Jaeger, N. I.; Niemann, W. *J. Chem. Soc., Chem. Commun.* **1991**, 678.

(31) Yarker, C. A.; Johnson, P. A. V.; Wright, A. C.; Wong, J.; Gregor, R. B.; Lytle, F. W.; Sinclair, R. N. *J. Non-Cryst. Solids* **1986**, *79*, 117.

(32) Gregor, R. B.; Lytle, F. W.; Sandstrom, D. R.; Wong, J.; Schultz, P. *J. Non-Cryst. Solids* **1983**, *55*, 27.

(33) Farges, F.; Brown Jr., G. E.; Rehr, J. J. *Geochim. Cosmochim. Acta*, in press.

Table 3. Catalytic Activity of Ti-Substituted (2 mol %) Molecular Sieves Prepared by Ambient Temperature Synthesis Using Different Templating Pathways^a

catalyst	MMA oxidation		styrene oxidation				2,6-DTBP oxidation ^c		H ₂ O ₂ decomp ^d
	conv (mol %)	select. MPV ^b (mol %)	conv. (mol %)	PhCHO select. (mol %)	epoxides elect. (mol %)	diol select. (mol %)	conv. (mol %)	quinones elect. (mol %)	conv (mol %)
TS-1	2.5	78	8.4	71	14	4.5	5		2.7
Ti-MCM-41 (S ⁺ I ⁻)	4.0	93	10	82	6.2	3.8	39	91	3.8
Ti-MCM-41 (S ⁺ X ⁻ I ⁺)	6.2	93	23	78	4.1	8.2	22	90	6.1
Ti-HMS (S ⁰ I ⁰)	6.8	93	28	77	4.7	9.6	55	91	2.2
anatase	0	0	2.6	0	64	29	4.5		13

^a TS-1 was prepared by prolonged hydrothermal synthesis as described in the Experimental Section. ^b MPV is methyl pyruvate. ^c Quinone selectivity is expressed as the cumulative selectivity of monomer quinone and dimer quinone. ^d H₂O₂ decomposition was determined by titration with a 0.1 N KMnO₄ aqueous solution of a "blank" reaction mixture (without substrate) of 30 mg of catalyst, and 30 mmol of 30 wt % H₂O₂ in 10 mL of H₂O that have been subjected to heating at 321 K for 2 h.

MCM-41 catalysts investigated to date were prepared by prolonged hydrothermal synthesis above 373 K using the electrostatic S⁺I⁻ pathway originally demonstrated by the pioneering work of Mobil.⁵ Here we compare the catalytic activity of Ti-MCM-41 and Ti-HMS samples prepared by *ambient temperature synthesis* using both S⁺I⁻ and S⁺X⁻I⁺ electrostatic templating pathways and the neutral S⁰I⁰ templating pathway, respectively. The catalytic performance of the samples was tested toward olefin and aromatic substrates of different size, such as the relatively small methyl methacrylate (MMA), styrene, and the bulky 2,6-di-*tert*-butylphenol (2,6-DTBP). The catalytic results are summarized in Table 3.

The mesoporous Ti-MCM-41 and Ti-HMS molecular sieves exhibit higher catalytic activity than microporous TS-1 for all reactions. The difference in catalytic activity between the mesoporous and microporous structures increases with increasing substrate size. The difference in catalytic activity is very small for the relatively small and elongated MMA molecule (2–2.5 times higher conversion for the mesoporous catalysts). However, as the substrate molecule becomes larger and more bulky (styrene and 2,6-DTBP) the difference in activity becomes much more pronounced. Thus, the difference in catalytic activity among Ti-MCM-41, Ti-HMS, and TS-1 reaches a maximum in the case of 2,6-DTBP (4–11 times higher conversion). This result is not surprising given the fact that the Ti-active centers are much more accessible in the larger mesopore size frameworks of Ti-MCM-41 and Ti-HMS. Due to the small micropore size of TS-1 (~6 Å), the large 2,6-DTBP substrate can not penetrate into the framework pores and therefore can not be transformed (only 5 mol % conversion). On the other hand, anatase (bulk titania) was completely inactive for MMA and styrene oxidation. Its catalytic activity for the conversion of the large 2,6-DTBP also is negligible (4.5 mol %).

The oxidation of MMA proceeds with higher selectivity to methyl pyruvate (MPV) over Ti-MCM-41 and Ti-HMS, but the microporous TS-1 affords slightly higher selectivity to epoxide (epoxide selectivity not included in Table 3). The tendency of TS-1 to oxidize olefins primarily to epoxides is well documented.³⁵ A similar trend also is observed for styrene oxidation. Generally, Ti-MCM-41 and Ti-HMS afford higher selectivity to diol, whereas more epoxide is produced over the microporous TS-1. The fact that the oxidation of MMA and styrene over Ti-MCM-41 and Ti-HMS proceeds selectively toward the alcohol derivative (through the epoxide intermediate) could be

a consequence of the more hydrophilic nature of the amorphous pore walls.

Notari *et al.* have reported that bulk titania or substituted silicas containing Ti–O–Ti bonds are not suitable for catalytic peroxide oxidation reactions because they selectively decompose H₂O₂.⁴ The comparison of the results for the H₂O₂ decomposition over our samples reveals a very interesting trend (Table 3, last column). In accordance with Notari *et al.* our anatase sample affords 13 mol % decomposition of H₂O₂. Both TS-1 and Ti-HMS exhibit lower H₂O₂ peroxide decomposition activity, whereas Ti-MCM-41 samples prepared by electrostatic S⁺I⁻ and S⁺X⁻I⁺ templating methods exhibit a higher tendency to decompose H₂O₂. Especially noteworthy is the higher degree of H₂O₂ decomposition by Ti-MCM-41 prepared by the acidic counterion-mediated pathway S⁺X⁻I⁺. This result is probably related to the pronounced tendency of the acidic S⁺X⁻I⁺ pathway to impede incorporation of Ti atoms in the silicate framework. All of our syntheses involving the counterion-mediated pathway required at least a 2–4-fold excess of Ti in the initial gel in order to achieve the desired Ti doping. It may be that the strongly acidic conditions used in the synthesis limit the incorporation of Ti atoms in the mesoporous framework.

A further comparison of the catalytic data reveals that S⁰I⁰-assembled Ti-HMS exhibits activity superior to electrostatically S⁺I⁻ and S⁺X⁻I⁺-assembled Ti-MCM-41 samples for all reaction systems. This enhanced activity for Ti-HMS is especially pronounced in the case of the large 2,6-DTBP. As shown by the data presented in Table 1, Ti-MCM-41 samples possess predominantly framework-confined mesoporosity and little or no significant textural mesoporosity.¹⁰ In contrast, Ti-HMS samples characteristically exhibit significant complementary textural or interparticle mesoporosity. The ratio of textural to framework-confined mesoporosity of Ti-HMS is usually equal to or higher than 1, whereas that of Ti-MCM-41 is usually close to zero. These differences in catalytic behavior of Ti-HMS and Ti-MCM-41 mesoporous molecular sieves are not due to differences in Ti siting, as judged from UV–vis and XANES data. We conclude, therefore, that the superior catalytic activity of Ti-HMS in liquid phase oxidations is most likely due to the presence of complementary textural mesoporosity that facilitates access of the framework-confined mesopores, especially by large organic substrates.

Conclusions

Hexagonal mesoporous titanasilicates containing 2 mol % Ti-substitution can be prepared by ambient temperature synthesis via three different surfactant templating approaches (S⁺I⁻, S⁺X⁻I⁺, and S⁰I⁰). Electrostatic S⁺I⁻ assembly of Ti-MCM-41 and neutral S⁰I⁰ assembly of Ti-HMS allow for almost complete incorporation of Ti in the mesoporous framework (at

(34) Sayari, A.; Karra, V. R.; Reddy, J. S.; Moudrakovski, I. L. in *Advances in Porous Materials*; Komarneni, Sh., Beck, J. S., Smith, D. M., Eds.; MRS Symposium Proceedings Series; MRS: Pittsburgh, 1995; Vol. 371, p 81.

(35) Kumar, S. B.; Mirajkar, S. P.; Pais, G. C. G.; Kumar, P.; Kumar, R. *J. Catal.* **1995**, *156*, 163.

a 2 mol % doping level), whereas electrostatic assembly of Ti-MCM-41 under acidic conditions via a counterion-mediated $S^+X^-I^+$ pathway impedes Ti incorporation. The incorporation of Ti in the anionic framework of MCM-41 materials and in the neutral framework of Ti-HMS mesopore frameworks is accompanied by an increase of the lattice parameter and the framework wall thickness. The framework mesopore size of the MCM-41 and HMS samples remains unaffected by the framework incorporation of Ti atoms. The degree of framework cross-linking of the electrostatic S^+I^- and $S^+X^-I^+$ -templated MCM-41 samples is significantly improved by Ti substitution as judged from the ^{29}Si MAS NMR data. The UV-vis and XANES results for calcined forms of Ti-MCM-41 and Ti-HMS provide evidence that (i) Ti species are incorporated and site-isolated into the framework structure, (ii) Ti atoms are predominantly in a tetrahedral coordination, but there is the possibility of some Ti sites in a five- or six-coordinated state. (Higher coordinated Ti sites most likely are generated by rehydration of some of the tetrahedrally coordinated sites), and (iii) the Ti sitings for the S^+I^- and $S^+X^-I^+$ Ti-MCM-41 and for $S^\circ I^\circ$ Ti-HMS are practically indistinguishable. This implies that the assembly pathway method has little or no effect on the Ti siting, at least when the Ti-MCM-41 and Ti-HMS samples are prepared under ambient temperature conditions.

A comparison of the catalytic results for the liquid phase peroxide oxidations of methyl methacrylate (MMA), styrene, and 2,6-di-*tert*-butylphenol (2,6-DTBP) reveals that Ti-MCM-41 and Ti-HMS exhibit catalytic activities higher than that of TS-1 for all reactions. The difference in activity between the mesoporous molecular sieve catalysts and microporous TS-1 increases with increasing substrate size. The activity difference is small for the relatively small MMA molecule, but as the substrate becomes larger, as in styrene and, especially, 2,6-

DTBP, the difference in activity becomes much more pronounced. This result is not surprising given the much more accessible Ti-active centers embedded in the larger mesopore size frameworks of Ti-MCM-41 and Ti-HMS. Due to the small micropore size of TS-1 ($\sim 6 \text{ \AA}$) the large 2,6-DTBP substrate cannot penetrate into the framework pores and therefore can not be transformed. $S^\circ I^\circ$ -assembled Ti-HMS exhibits greater catalytic activity than the Ti-MCM-41 materials assembled by electrostatic S^+I^- and $S^+X^-I^+$ pathways. The superior performance of Ti-HMS is especially pronounced in the case of the large 2,6-DTBP. On the basis of UV-vis and XANES data, these differences in catalytic behavior of Ti-HMS and Ti-MCM-41 cannot be attributed to differences in Ti coordination environment. Because Ti-HMS has thicker framework walls than Ti-MCM-41, an enhancement in the fraction of surface Ti sites cannot be responsible for the greater activity of Ti-HMS. The most distinguishing structural feature between Ti-HMS and Ti-MCM-41 is the greater interparticle (textural) mesoporosity for Ti-HMS. This complementary textural mesoporosity most likely facilitates substrate transport and access to the framework-confined mesopores, thus enhancing the catalytic efficiency of Ti-HMS.

Acknowledgment. The partial support of this research by the National Science Foundation (Grants CHE-9224102 and CHE-9633798) is gratefully acknowledged. The XANES measurements were carried out at the Stanford Synchrotron Radiation Laboratory (SSRL) supported by the Chemical Division of the U.S. Department of Energy (DOE). M.F. thanks the Alexander von Humboldt Foundation for a Feodor Lynen Research Fellowship.

JA960594Z